Nightside geosynchronous magnetic field response to interplanetary shocks: Model results

T. R. Sun,[1,2] C. Wang,[1] H. Li,[1,2] and X. C. Guo[1]

Received 31 August 2010; revised 9 December 2010; accepted 29 December 2010; published 19 April 2011.

[1] Inspired by the fact that spacecraft at geosynchronous orbit may observe an increase or decrease in the magnetic field in the midnight sector caused by interplanetary fast forward shocks (FFS), we perform global MHD simulations of the nightside magnetospheric magnetic field response to interplanetary (IP) shocks. The model reveals that when a FFS sweeps over the magnetosphere, there exist mainly two regions: a positive response region caused by the compressive effect of the shock and a negative response region which is probably associated with the temporary enhancement of earthward convection in the nightside magnetosphere. IP shocks with larger upstream dynamic pressures have a higher probability of producing a decrease in B_z that can be observed in the midnight sector at geosynchronous orbit, and other solar wind parameters such as the interplanetary magnetic field (IMF) B_z and IP shock speed do not seem to increase this probability. Nevertheless, the southward IMF B_z leads to a stronger and larger negative response region, and a higher IP shock speed results in stronger negative and positive response regions. Finally, a statistical survey of nightside geosynchronous B_z response to IP shocks between 1998 and 2005 is conducted to examine these model predictions.

Citation: Sun, T. R., C. Wang, H. Li, and X. C. Guo (2011), Nightside geosynchronous magnetic field response to interplanetary shocks: Model results, *J. Geophys. Res.*, *116*, A04216, doi:10.1029/2010JA016074.

1. Introduction

[2] The magnetospheric magnetic field configuration under different solar wind conditions is one of the key subjects of space weather studies. Among various solar wind disturbances which introduce perturbations to the magnetospheric magnetic field, interplanetary fast forward IP shocks are frequently observed solar wind disturbances which bring about significant changes of solar wind parameters in a short time scale.

[3] When the IP shock impinges on the magnetopause, an impact force is applied to the plasma there. *Tamao* [1964] provided an ideal picture that a local source causes isotropic compressional waves in uniform cold plasma. More realistically, for a tangential discontinuity magnetopause, the interaction with an IP shock launches a transmitted fast shock into the magnetosphere [*Shen*, 1973; *Grib et al.*, 1979; *Zhuang et al.*, 1981]. Propagation and reflection of the transmitted shock in the dayside magnetosphere was studied by *Samsonov et al.* [2007] in detail. Based on MHD simulations, *Ridley et al.* [2006] implied that when the shock passes the terminator, it flows around the boundary and eventually fills in the near-Earth tail region. Statistical study on shock propagation in the nightside magnetosphere was done by *Andréeová et al.* [2008]. According to their analysis of more than 40 events, disturbance speeds both across the terminator and in the nightside magnetosphere are dependent on shock speed and upstream dynamic pressure.

[4] Propagation of the disturbance front, which is launched by impingement of the shock on the magnetopause, introduces magnetic field perturbations to the magnetosphere. Compression of the magnetic field in the dayside magnetosphere is not only widely observed but also reproduced by MHD simulations [e.g., *Samsonov et al.*, 2007; *Andréeová and Přech*, 2007]. However, nightside magnetic field responses are more complicated. *Li et al.* [2003] concluded that both the magnetic and electric fields in the magnetotail can respond globally to IP shocks and presented a case where the magnetic field response was positive. *Andréeová et al.* [2008] found that only weak disturbances of magnetic field were recorded by both Polar and Cluster based on case study of the magnetospheric response to a double shock. They also performed an MHD simulation of this case which predicted an insignificant change of the magnetic field at the position of Polar, as well as a weak increase at the position of Cluster 1. Recently, *Wang et al.* [2009] reported that geosynchronous magnetic field on the nightside can sometimes drop sharply in response to an IP shock according to a statistical study of FFS cases between 1998 and 2005. By using MHD simulations, *Wang et al.* [2010] performed case studies of the response observed by the GOES spacecraft at geosynchronous orbit near midnight to two IP shocks passing Earth. One shock produces a decrease in B_Z (a negative response)

[1]State Key Laboratory of Space Weather, Center for Space Science and Applied Research, Chinese Academy of Sciences, Beijing, China.

[2]Also at Department of Space Physics, Graduate University of the Chinese Academy of Sciences, Beijing, China.

0148-0227/11/2010JA016074

Table 1. List of MHD Parameters for Six Simulated IP Shocks[a]

Case	P_{dup} (nPa)	N_{up} (cm^{-3})	V_{xup} (km/s)	B_{zup} (nT)	T_{up} (eV)	V_s (km/s)	x_{b0} (R_E)	dB_{zgeo} (nT)
1	0.45	3	300	0	7	600	−9.3 ± 0.4	9.3
2	6.26	15	500	0	7	600	−6.6 ± 0.4	−17.9
3	6.26	15	500	5	7	600	−6.9 ± 0.4	−12.1
4	6.26	15	500	−5	7	600	−6.4 ± 0.4	−20.9
5	0.45	3	300	0	7	450	−9.1 ± 0.4	5.3
6	0.45	3	300	0	7	900	−9.0 ± 0.4	21.3

[a]P_{dup}, N_{up}, V_{xup}, B_{zup}, and T_{up} are dynamic pressure, number density, x component velocity, z component magnetic field, and temperature upstream of the shocks, respectively. V_s is shock speed. The initial position of the boundary between positive and negative response regions on the Sun-Earth line is denoted by x_{b0}, and it has 0.4 R_E uncertainty (due to mesh spacing). B_z variation at the midnight point of the geosynchronous orbit is represented by dB_{zgeo}.

and the other an increase in B_Z (a positive response). They concluded that both positive and negative response regions form on the nightside of the magnetosphere after the passage of an IP shock, and the negative response region expands toward Earth after its formation. Consequently, the spacecraft at geosynchronous orbit in the nightside sector may observe an increase or decrease of the magnetic field depending on which region it is in. However, the affect of IP shock properties (such as the dynamic pressure, speed, magnetic field direction etc.) on the nightside magnetospheric response has not been studied. In this paper, we will conduct a series of numerical test runs to investigate these factors which may be significant for the magnetospheric response in a systematic way. Finally, a statistical survey is performed to examine the model predictions. A brief introduction to the MHD model and data sources is given in section 2. The model results and the statistical study are presented in sections 3 and 4, respectively. The summary is given in section 5.

2. Numerical Model and Data Sources

[5] The numerical model used in this study is the same as described in our previous work [*Wang et al.*, 2010]. We adopted the global MHD simulation code developed by *Hu et al.* [2007], which employs an extended Lagrangian version of the piecewise parabolic method (PPMLR) [*Collela and Woodward*, 1984]. All numerical cases are run under the following assumptions: (1) the solar wind is along the Sun-Earth line, (2) the Earth's dipole moment is due southward, and (3) the ionosphere is assumed uniform with a fixed Pedersen conductance and a zero Hall conductance. The solution domain is $-300 \le x \le 30$ R_E and $-150 \le y, z \le 150$ R_E in terms of the GSM coordinate, and a spherical shell with a radius of 3 R_E is set to be the inner boundary of the magnetosphere. The numerical box is divided into 160 × 162 × 162 grid points, with a minimum grid spacing of 0.4 R_E.

[6] In order to introduce a shock, we first choose an initial interplanetary state as the upstream condition of the shock and calculate more than 7 h (physical time) so that the system can reach a quasi-steady state. Then, the MHD parameters at the inflow boundary are changed to downstream ones, which are obtained using the shock speed and Rankine-Hugoniot relations. Consequently, a shock is launched at $T = 0$ min. The model time resolution is 9.35 s.

[7] For the statistical study in an attempt to check the model predictions, 16 s time resolution IMF data and 64 s time resolution proton number density, velocity, and temperature from ACE satellite (http://cdaweb.gsfc.nasa.gov/istp_public/) are used to analyze IP shocks. In order to obtain the temporal variations of geosynchronous magnetic field, we adopt 1 min resolution data from GOES 8, 9, 10 and 12 (http://cdaweb.gsfc.nasa.gov/istp_public/).

3. Model Results

[8] As will be seen in section 3.1, the model results show that when a FFS sweeps over the magnetosphere, there always exist positive response and negative response regions in the nightside magnetosphere. In order to describe the interaction in a quantitative way, we introduce a parameter x_b, defined as the position of the interface between the positive and negative response regions along the x axis after the impact of an IP shock. As would be expected, the parameter x_b is a function of time. The initial value is x_{b0} at time t_0 when both regions form initially in response to IP shocks:

$$x_b = x_b(t), t \ge t_0 \tag{1}$$

$$x_{b0} = x_b(t_0) \tag{2}$$

According to case studies in the work by *Wang et al.* [2010], the parameter x_{b0} determines what kind of B_z variation a geosynchronous spacecraft will observe at the midnight point: if $x_{b0} < -6.6$ R_E, an increasing B_z will be detected right after the passage of the IP shock, and if $x_{b0} \ge -6.6$ R_E, a decreasing B_z will be detected instead. In this section, we will present a typical numerical example in detail first, and then we examine numerically the dependence of the parameter x_{b0} on three shock parameters, i.e., the upstream solar wind dynamic pressure P_{dup}, the upstream IMF Bz component B_{zup}, and the shock speed.

[9] Table 1 presents 6 different IP shocks investigated in this study, with the shock normal and propagation direction parallel to the Sun-Earth line. MHD parameters not listed in Table 1 (i.e., B_{xup}, B_{yup}, V_{yup}, and V_{zup}) are set zero. Cases 1 and 2 are used to compare the negative and positive response regions under different upstream solar wind dynamic pressures; cases 3 and 4 are used to study the effect of IMF B_{zup}, and the influence of the shock speed is investigated by cases 5 and 6.

3.1. Nightside Magnetic Field Response: An Example

[10] By analyzing convection in the nightside magnetosphere, *Wang et al.* [2010] proposed that the temporary earthward flow introduced by impingement of the IP shock

on nightside magnetopause might be responsible for the formation of the negative response region. Here we present simulation result of case 1 to further examine the convection and the time evolution of nightside magnetic field. Since the solar wind parameters in case 1 are symmetric about the equatorial and meridian plane, the negative and positive response regions in the nightside magnetosphere are also symmetric. Thus the example presented in this study is relatively easier to do the analysis than the real cases of *Wang et al.* [2010].

[11] Figure 1 displays velocity vectors and contours of $d|B_z|$, defined by equation (3) below, in the nightside magnetosphere on the equatorial plane.

$$d|B_z| = |B_z(t)| - |B_z(0)|, \tag{3}$$

Here, $B_z(t)$ and $B_z(0)$ represent z component magnetic field at times $T = t$ and $T = 0$, respectively. Process of the magnetic field response starting from $T = 5.61$ min when the IP shock flows by the terminator until it passes the near-Earth magnetotail at $T = 10.60$ min is illustrated at a 37.4 s time cadence. Figure 1a shows that the disturbance flow introduced by the impingement of the IP shock on the dayside magnetopause roughly propagates tailward near the terminator. Fronts of the flow bulge toward the tail in both the upper ($y > 0$) and lower ($y < 0$) sectors, corresponding to fronts of the compressional signal of the magnetic field. As the IP shock propagates further tailward at $T = 6.23$ min, the flow launched near the flanks of the magnetopause clearly possesses a y component. According to ideal MHD theory, if a flow is launched at a location (point A) and propagates in a direction perpendicular to the background magnetic field, the transportation of the magnetic flux from point A in the same direction is also aroused following the frozen-in-field theorem, which leads to decrease of the magnetic field magnitude at point A if no extra flux can compensate the loss. In Figure 1b, the flux transports from places near the magnetopause toward both the magnetotail and the Sun-Earth line, and this will result in two negative response regions in the magnetosphere later in Figure 1c. At the same time, disturbance fronts in the upper and lower sectors spread to the Sun-Earth line. The compressive effect of the IP shock leads to formation of a positive response region near Earth, which covers the midnight point of the geosynchronous orbit denoted by the white star in Figure 1c. At $T = 6.86$ min when the flows further converge toward the x axis, a weak earthward flow takes shape near the Sun-Earth line. The magnetic field strength in the positive response region keeps increasing as this newly formed flow brings in magnetic flux from the tail, which, on the other hand, leads to the formation of another negative response region at $x \approx -14 \sim -9\ R_E$ at $T = 7.48$ min (see Figure 1d). The entire system keeps developing in the following minutes, and finally three negative response regions inside the magnetosphere merge into one at $T = 8.26$ min (not shown). During this merging process, the Earth-side boundary of the negative response region in the vicinity of the x axis (marked by black lines in Figures 1d and 1e) slightly moves toward Earth. While after merging, the negative response region expands earthward due to the greatly enhanced earthward flow (Figures 1f–1h). The positive response region retreats back since the magnetic flux transported from the tail diverges at $x \approx -8 \sim -7\ R_E$ toward the flanks, instead of piling up in the inner magnetosphere. This results in a slight decrease of B_z at the midnight point of the geosynchronous orbit after it reaches the maximum, as was indicated by *Wang et al.* [2010, Figure 2]. On the tail side of the merged negative response region in Figure 1h, the front of the compressional signal propagates tailward as a unity, forming another positive response region. However, considering that the magnitude of the magnetic field remarkably drops toward the tail, the compression of the magnetosphere in this region is much weaker than that near Earth. As time passes by, the fluid near Earth gradually ceases (Figure 1i).

[12] Time variation of the interface between the positive and negative response regions along the x axis (x_b) is plotted in Figure 2. This interface moves earthward first, and then stays almost at the same place. According to the definition in equation (2), the parameter $t_0 \approx 7.48$ min in this case, since the negative response region near the x axis originally forms at this time. However, considering that x_b does not vary significantly during the merging process of the three negative response regions (from $-9.3\ R_E$ to $-8.8\ R_E$), using the boundary position right after the emerging process as a criteria is also reasonable, i.e.,

$$x_{b0} = -9.3\, R_E \approx x_b(8.26\, \mathrm{min}) = -8.8 R_E. \tag{4}$$

Since $x_{b0} < -6.6\ R_E$ for case 1, a geosynchronous orbit satellite at the midnight point will observe a positive B_z response (Figure 3, top).

3.2. Nightside Magnetic Field Responses to Shocks With Different Parameters

[13] In this section, we investigate three shock parameters which might affect x_{b0}, and try to predict nightside geosynchronous B_z responses to IP shocks with different characters.

3.2.1. Influence of Upstream Dynamic Pressure

[14] Cases 1 and 2 are run to study the nightside magnetospheric B_z response to IP shocks with different P_{dup}. Figure 3 depicts time variation of B_z ($dB_z = B_z(t) - B_z(0)$) at the midnight point of the geosynchronous orbit for both cases. For case 1 with $P_{dup} = 0.45$ nPa, the magnetic field z component B_z at that position exhibits a sudden increase of approximately 9.3 nT right after the passage of the shock, and the ascending process lasts about 3 min. By contrast, a sharp drop of B_z is presented in case 2, a case with a much larger upstream dynamic pressure: $P_{dup} = 6.26$ nPa. In this case, B_z barely changes before $T = 7.79$ min, and rapidly decreases by -17.9 nT within next 3 min. We thereby conclude that satellite at the midnight point of geosynchronous orbit tends to observe increasing/decreasing B_z if the IP shock has small/large P_{dup}. In other words, IP shocks with larger upstream dynamic pressures have a higher probability of producing a decrease in B_z that can be observed in the midnight sector at geosynchronous orbit.

[15] Figure 4 is plotted to illustrate influence of P_{dup} on x_{b0} and the introduced convection on the nightside magnetosphere, which might be responsible for different location of the negative response region. Figures 4a and 4d are contours of $d|B_z|$ on the equatorial plane for cases 1 and 2 when the negative response region near the x axis initially forms, with the white dashed and solid lines marking the

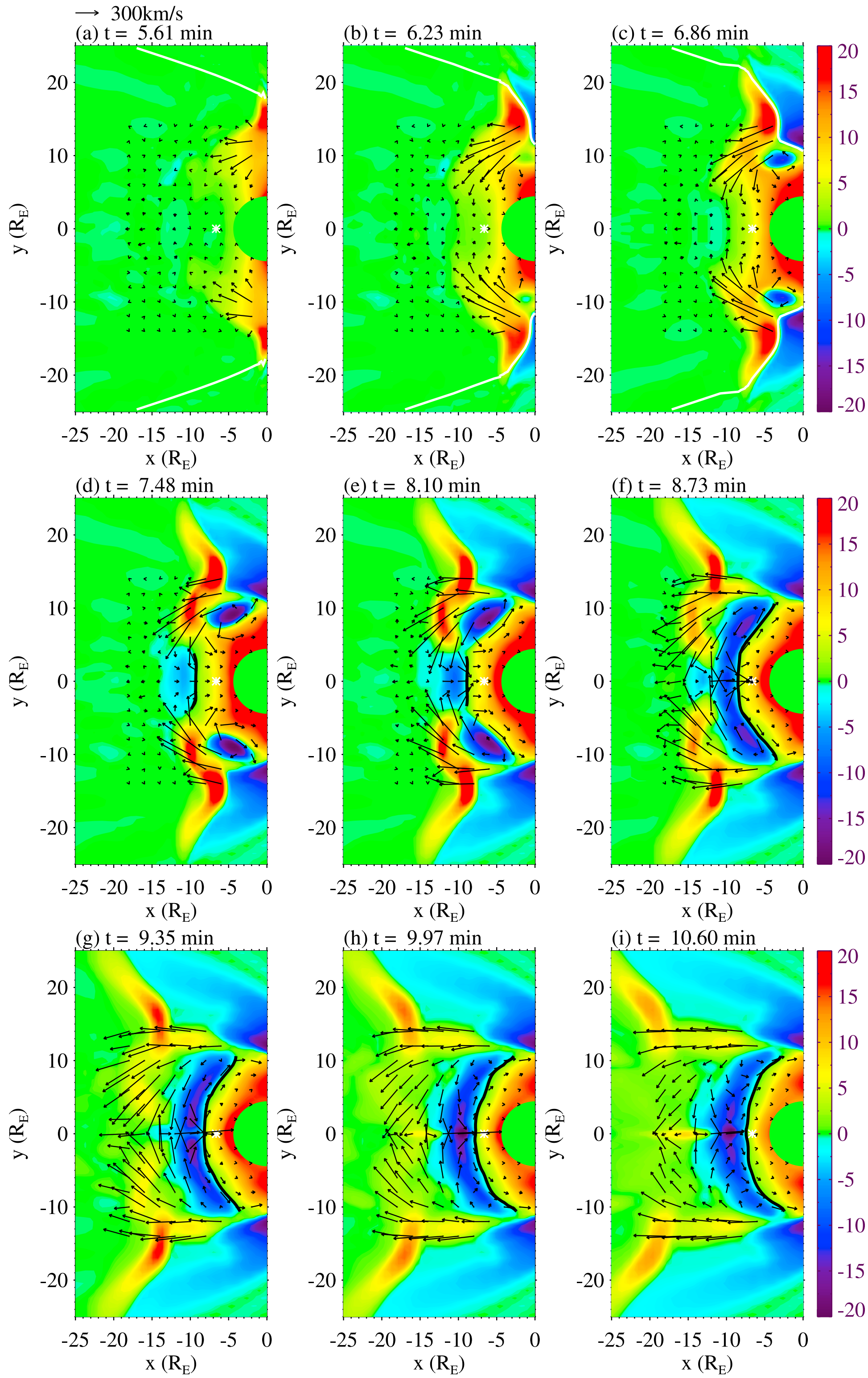

Figure 1. B_z response and convection in the nightside magnetosphere of case 1 (P_{dup} = 0.45 nPa). Contours of $d|B_z|$ on the equatorial plane from T = 5.61 min to 10.60 min are plotted at a 37.4 s cadence. The arrows show velocity vectors with the scale of the magnitudes represented by the arrow above Figure 1a. The white star marks the midnight point of geosynchronous orbit, and the white line in Figures 1a–1c is the magnetopause. The boundary between the negative and positive response regions is shown by the black line in Figures 1d–1i.

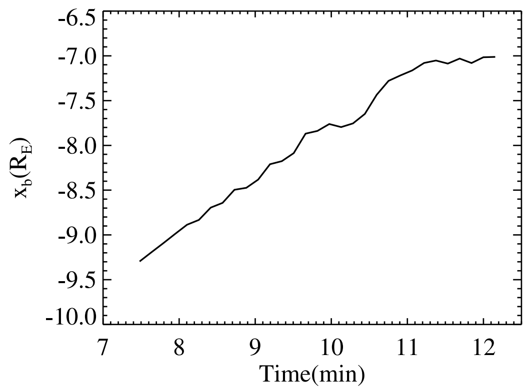

Figure 2. Time evolution of the interface between the positive and negative response regions along the x axis (x_b) for case 1. The IP shock is introduced at $T = 0$ min at the inflow boundary.

magnetopause before and after the impact of the IP shock, respectively. Figures 4b and 4e show contours of $d|B_z|$ for both cases on the equatorial plane when the amplitudes of B_z variation in Figure 3 reach their maxima, and Figures 4c and 4f are plots on the meridian plane at the same time. The White star marks the midnight point of geosynchronous orbit. Figure 4b manifests that for case 1, the white star is enveloped by the positive response region near Earth, with the negative response region far on the tail side. However, the white star in Figure 4e is covered by the blue region instead, which is much closer to Earth. Figures 4a and 4d, as well as Table 1, show that P_{dup} affects x_{b0} significantly: the initial boundary is much closer to Earth if P_{dup} is enhanced. As indicated by Figure 1b, the disturbance flow launched near the flanks of the magnetopause has both an x component and a y component. Consequently, those disturbance fronts in the upper ($y > 0$) and lower ($y < 0$) sectors will converge and form a negative response region at a place closer to Earth, if the distance between two flank points of the magnetopause before the arrival of the IP shock is shorter. The simulation results show that a larger P_{dup} corresponds to a shorter distance between the flanks (see the white dashed lines in Figures 4a and 4d), and therefore corresponds to an x_{b0} closer to Earth. In addition, Figures 4c and 4f reveal that the thickness of the negative response region along the z axis has no apparent differences in both cases, and thus we do not focus on responses in the meridian plane in this paper.

3.2.2. Influence of Upstream IMF B_z

[16] Case 3 with northward IMF B_{zup} and case 4 with southward IMF B_{zup} are selected to study the effect of the upstream B_z. Figures 5a and 5c plot contours of $d|B_z|$ on the equatorial plane for both cases when the negative response region near the x axis initially forms, and Figures 5b and 5d are plots when the amplitudes of dB_z at the midnight point of geosynchronous orbit almost reach their maxima. Nightside convection is shown by arrows in Figures 5a and 5b for case 3. Since the nightside magnetosphere has large background convection under southward IMF conditions and we concentrate on the part the IP shock introduces, thus the background convection patterns are subtracted and only the residual velocity is displayed in Figures 5c and 5d for case 4. The initial position of the boundary x_{b0} is close to the midnight point of geosynchronous orbit for both cases, and the negative response region develops toward Earth afterward (Figures 5b and 5d), indicating that under relatively higher P_{dup} conditions, satellite at the midnight point of geosynchronous orbit will detect a negative response of B_z regardless of the direction of IMF B_{zup}. This viewpoint is also clarified by the data in Table 1, which shows that x_{b0} is only 0.5 R_E closer to Earth in case 4 than case 3. Considering that minimum grid space of the MHD code is 0.4 R_E, this difference is not so significant. As described in section 3.2.1, the value of x_{b0} is affected by the distance between two flank points of the magnetopause before the arrival of the IP shock. Since the white dashed lines in Figures 5a and 5c imply that the distance between flank points does not vary significantly with the direction of IMF B_{zup} (consistent with the conclusion drawn by *Shue et al.* [1997]), values of x_{b0} for both cases approximately equal.

[17] Table 1 also reveals that amplitude of dB_{zgeo} is larger when IMF B_{zup} is southward, in agreement with Figures 5b and 5d, which presents a wider and stronger negative response region in case 4 than that in case 3. Actually, for case 4, the southward IMF B_z increases across the IP shock front, and consequently, the reconnection in the magnetotail is enhanced after the arrival of the shock. This process as

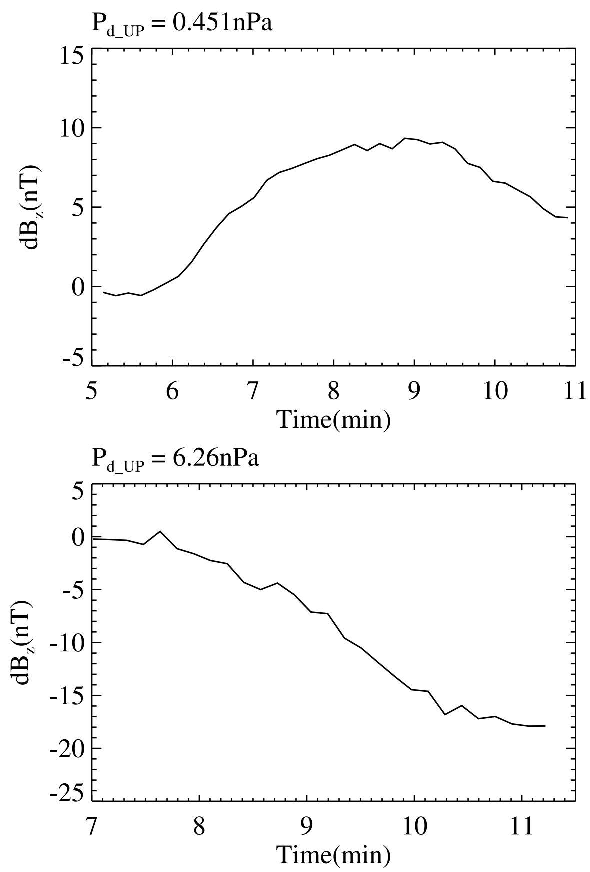

Figure 3. Time variation of the magnetic field z component (dB_z) at the midnight point of the geosynchronous orbit for (top) case 1 with P_{dup} = 0.45 nPa and (bottom) case 2 with P_{dup} = 6.26 nPa. IP shocks are introduced at $T = 0$ min at the inflow boundary for both cases.

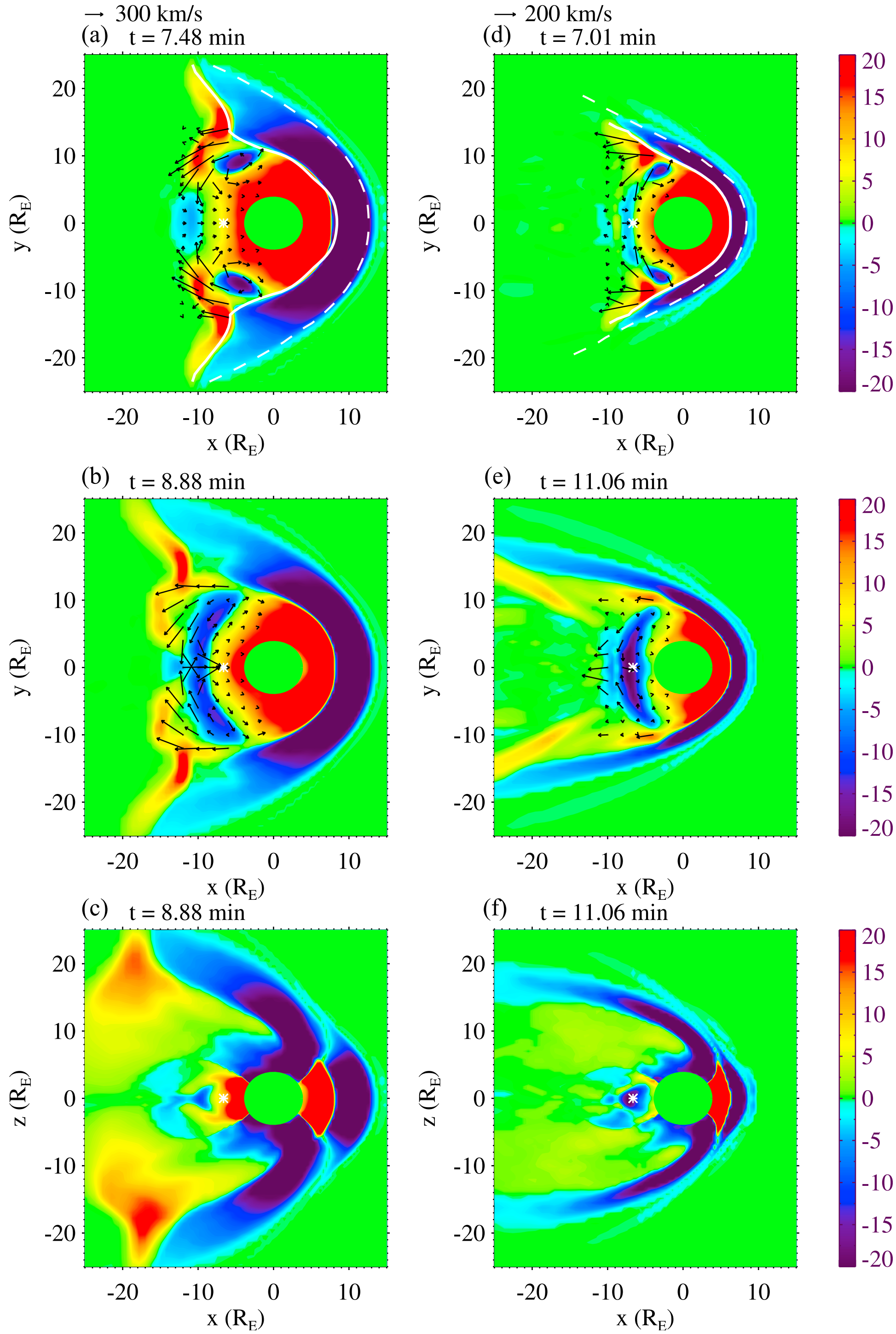

Figure 4. Contours of $d|B_z|$ and convection vectors for (a-c) case 1 with P_{dup} = 0.45 nPa and (d-f) case 2 with P_{dup} = 6.26 nPa. Figures 4a and 4d are plots on the equatorial plane when the negative response region near the x axis initially forms. The white dashed and solid lines mark the magnetopause before and after the impact of the IP shock, respectively. Figures 4b and 4e are plots on the equatorial plane when amplitudes of dB_z at the midnight point of the geosynchronous orbit reach their maxima, and Figures 4c and 4f are contours on the meridian plane at the same time. The white stars denote the midnight point of the geosynchronous orbit.

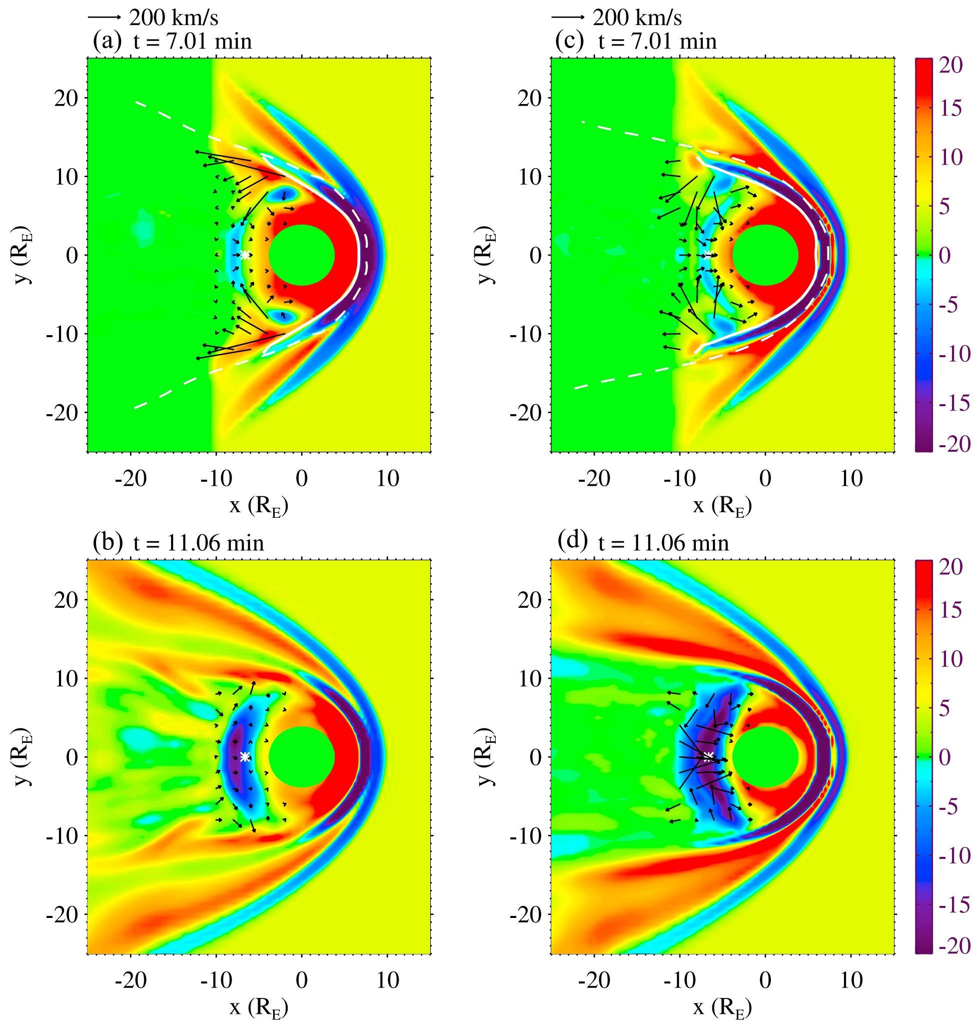

Figure 5. Contours of $d|B_z|$ on the equatorial plane for (a and b) case 3 and (c and d) case 4 (P_{dup} = 6.26 nPa). Figures 5a and 5c are plots for cases 3 and 4 when the negative response region near the x axis initially forms at T = 7.01 min, and Figures 5b and 5d are pictures for the two cases when amplitudes of dB_z at the midnight point of geosynchronous orbit almost reach their maxima at T = 11.06 min. Arrows in Figures 5a and 5b are convection vectors for case 3, while in Figures 5c and 5d they show residual velocity for case 4, with the background convection patterns subtracted. The white dashed and solid lines depict the magnetopause before and after the impact of the IP shock, respectively, and white stars mark the midnight point of the geosynchronous orbit.

well as the temporary earthward flow both contributes to the formation of the negative response region in case 4, and thus leads to a wide and deep blue region in Figure 5d.

3.2.3. Influence of Shock Speed

[18] In order to examine the influence of shock speed on nightside magnetospheric B_z responses, cases 5 and 6 are run for IP shocks with different speed (450 versus 900 km/s). The position x_{b0} does not vary dramatically along with the shock speed, however a larger shock speed corresponds to a stronger B_z response at the midnight point of geosynchronous orbit (see Table 1). That is to say, the sign of dB_{zgeo} will not change if the shock speed increases, but the amplitude of the magnetic variation will become larger.

[19] This is also illustrated by Figure 6, which displays contours of $d|B_z|$ and convection vectors for cases 5 and 6 when the negative response region near the x axis initially forms (Figures 6a and 6c) and when the amplitudes of dB_z at the midnight point of the geosynchronous orbit almost reach their maxima (Figures 6b and 6d). The introduced flow in the nightside magnetosphere is dramatically enhanced if the shock speed is increased and therefore, both the loss of magnetic flux in the negative response regions and the piling up of field lines in the positive response regions are enhanced, resulting in larger amplitude of dB_{zgeo}. The white dashed lines in Figures 6a and 6c demonstrate that for both cases, the distances between flanks of the magnetopause before the arrival of the IP shock are the same, in that both shocks have identical upstream parameters. This explains the nearly stable x_{b0} for cases with different shock speeds.

[20] In a word, cases 1–6 reveal that the parameter x_{b0}, which determines what kind of the magnetic field z component B_z variation a satellite at geosynchronous orbit in the

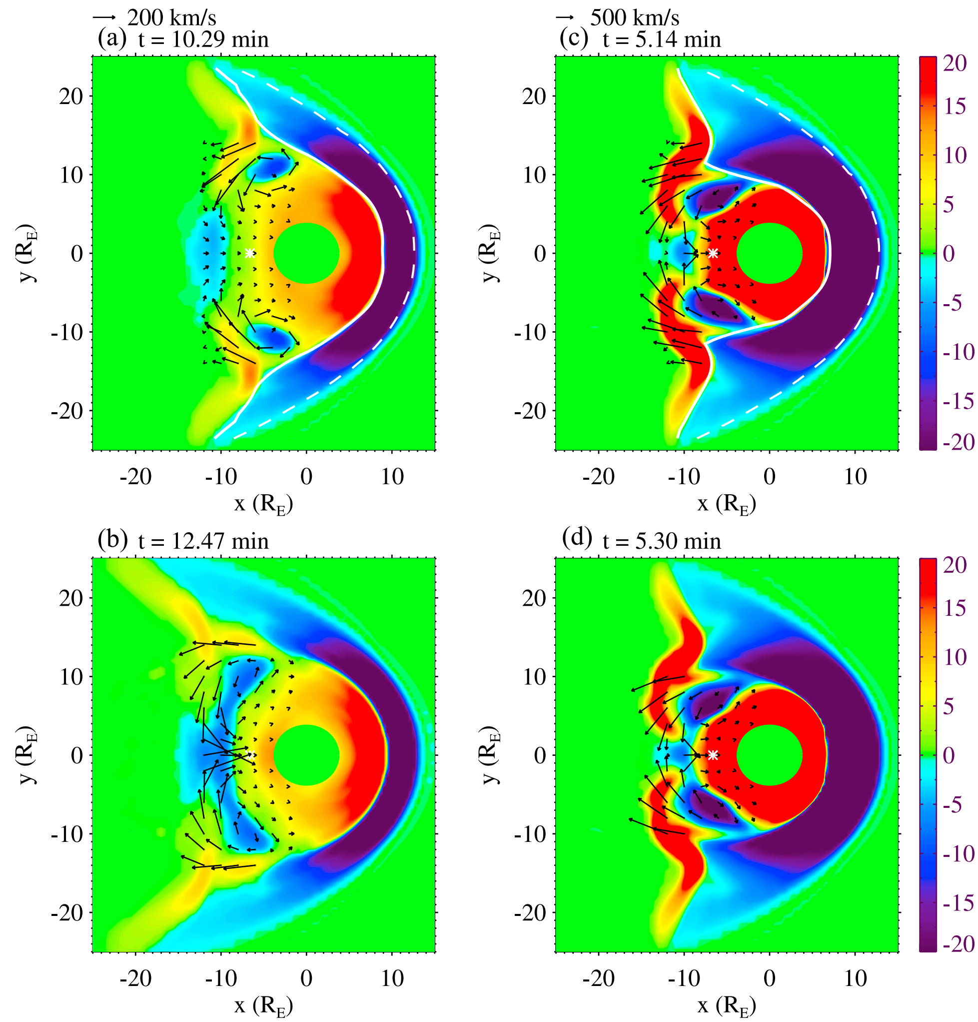

Figure 6. Contours of $d|B_z|$ and convection vectors on the equatorial plane for (a and b) case 5 and (c and d) case 6 (P_{dup} = 0.45 nPa). Figures 6a and 6c are plots for cases 5 and 6 when the negative response region near the x axis initially forms (T = 10.29 min for case 5 and T = 5.14 min for case 6), and Figures 6b and 6d are plots for both cases when amplitudes of dB_z at the midnight point of geosynchronous orbit almost reach their maxima (T = 12.47 min for case 5 and T = 5.30 min for case 6). The white dashed and solid lines depict the magnetopause before and after the impact of the IP shock, respectively, and white stars denote the midnight point of the geosynchronous orbit.

midnight sector will observe, is an increasing function of P_{dup} and almost independent of the IMF B_{zup} and the shock speed.

4. Statistical Study

[21] In an attempt to check the model predictions mentioned above, we present a statistical study of the nightside geosynchronous B_z responses to IP shocks from 1998 to 2005. Events with at least one of the GOES satellites located in the midnight sector (0000~0300 LT and 2100~2400 LT) of the geosynchronous orbit after the arrival of the IP shock are selected and only those without magnetic storm, i.e., $Dst > -50$ nT (http://wdc.kugi.kyoto-u.ac.jp/), are chosen for the present study. We further required events in which the B_z (in GSM coordinate) variation be at least greater than 2 nT to be included, which results in 54 events (25 positive response events and 29 negative response ones) being selected. In order to examine the relationship between the nightside B_z responses and the upstream IMF B_z orientation given by simulation results, an additional requirement that both the upstream and downstream IMF B_z are of the same sign is imposed, since we do not consider the inversion of IMF B_z in the MHD simulation for simplicity. Consequently, 44 events are left for this particular goal. It should be noticed that this additional criterion is different from the one used by *Wang et al.* [2009], where the southward IMF B_z cases were selected by requiring that IMF B_z either upstream or downstream of the IP shock is southward. For each IP shock, Magnetic Coplanarity (MC), Velocity Coplanarity (VC), minimum variance analysis (MVA) and the Rankine-Hugoniot method are used to determine the shock speed.

[22] Figure 7 shows the dependence of the nightside B_z response on the upstream solar wind dynamic pressure (Figure 7a), the upstream IMF B_z (Figure 7b) and the shock

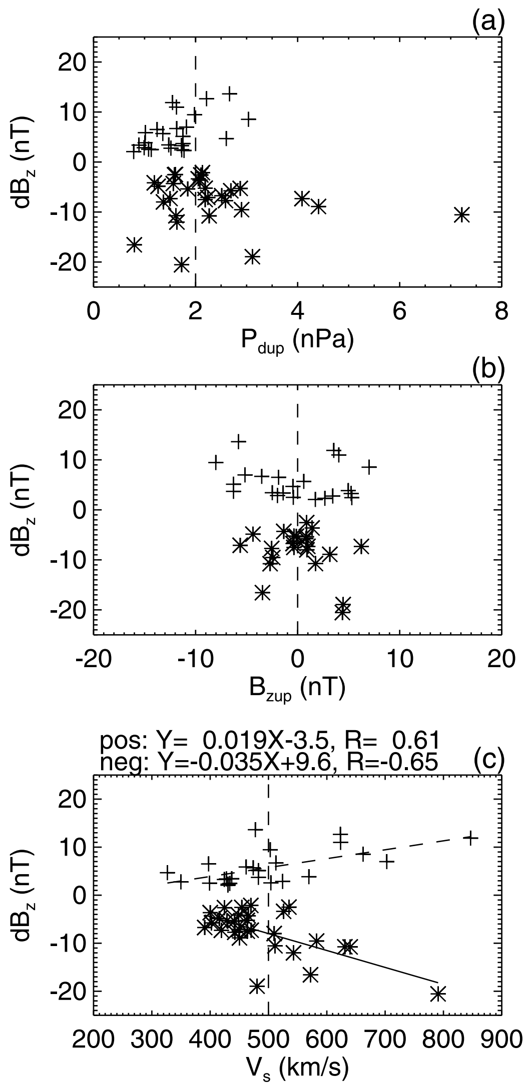

Figure 7. Statistics of midnight side B_z responses to IP shocks. (a) Dependence of dB_z on P_{dup}. (b) Relationship between dB_z and IMF B_{zup}. (c) B_z responses to IP shocks with different shock speeds. In all three plots, crosses represent positive response events, and stars denote negative response events. Dashed and solid lines in Figure 7c show linear fits for positive and negative response events, respectively.

speed (Figure 7c). Figure 7a demonstrates that 21 events out of the 33 ones with P_{dup} < 2 nPa (or 64%) show positive response while 17 events out of 21 ones with P_{dup} > 2 nPa (or 81%) exhibit negative response. The average P_{dup} of positive response events is 1.61 nPa, in comparison with an average of 2.32 nPa for negative response events. This implies that a satellite in the midnight sector of the geosynchronous orbit tends to observe decreasing/increasing B_z if P_{dup} is large/small, in agreement with the model predictions. As would be expected, some exceptions exist in Figure 7a due to other factors besides the upstream dynamic pressure. A possible factor might be the deviation of the shock normal from the Sun-Earth line, which introduces the complexity of the locations of negative response regions. The tilt angle of the dipole axis, which is set zero in the MHD model for simplicity, may also contributes. Nevertheless, based on the major characteristic of the statistical study as well as the simulation results, the upstream solar wind dynamic pressure P_{dup} is probably the main factor determining the sign of nightside geosynchronous dB_z. Figure 7b reveals that almost the same number of positive and negative response events were recorded by GOES for both the southward IMF B_{zup} (12 positive response versus 11 negative response) and northward IMF B_{zup} (10 positive response versus 11 negative response). Whether the GOES spacecraft observes an increasing or decreasing B_z in the midnight sector has no obvious association with the sign of IMF B_{zup}, provided that no inversion of B_z exists across the IP shock front. This conclusion once again supports the model predictions. MHD simulation also predicts that larger amplitude of dB_z will be recorded under southward IMF B_{zup} for negative response cases, which is not supported by the present statistical study. This might be resulted from the possibility that influence of IMF B_{zup} direction on the amplitude of dB_z is embedded in other effects, and more cases are needed to do the statistical study. Figure 7c shows that almost the same number of positive and negative response events were observed for both higher shock speeds (10 positive response events versus 10 negative response events when V_s > 500 km/s) and lower ones (15 positive response versus 19 negative response when V_s < 500 km/s), implying that what kind of the B_z variation is almost independent of the shock speed, which is just what the model predicts. Furthermore, both model predictions and the statistical results (Figure 7c) show that the higher IP shock speed leads to the larger amplitude of the change of the magnetic field (dB_z).

5. Summary and Conclusion

[23] Inspired by the fact that spacecraft at geosynchronous orbit may observe an increase or decrease in the magnetic field in the midnight sector caused by interplanetary fast forward shocks (FFS), we perform global MHD simulations of the nightside magnetospheric magnetic field response to interplanetary (IP) shocks.

[24] Due to the temporarily enhanced flow in the nightside magnetosphere after the impingement of an IP shock, three negative response regions form in the magnetotail and then quickly merge together. On the Earth side there forms a positive response region, resulting from the compressional effect of the shock. The initial position of the boundary between positive and negative response regions along the x axis (x_{b0}) determines what kind of B_z variation a satellite will observe at geosynchronous orbit in the night sector. The upstream solar wind dynamic pressure affects x_{b0} significantly; that is, large/small P_{dup} corresponds to an initial boundary close to/far away from Earth, while IMF B_{zup} and shock speed have no significant influence on x_{b0}. That is, IP shocks with larger upstream dynamic pressures have a higher probability of producing a decrease in B_z that can be observed in the midnight sector at geosynchronous orbit, and other solar wind parameters such as the interplanetary magnetic field(IMF) B_z and IP shock speed seem not increase this probability. Nevertheless, the negative response region becomes stronger and larger if the IMF B_{zup} points southward, resulting in larger amplitude of

the change of geosynchronous magnetic field (dB_{zgeo}) for negative response cases. Both the positive and negative response regions become stronger if the shock speed increases, leading to larger amplitude of dB_{zgeo}.

[25] Finally, a statistical survey of nightside geosynchronous B_z response to IP shocks between 1998 and 2005 is conducted to examine these predictions. Generally speaking, the model predictions are in good agreement with the statistically results.

[26] **Acknowledgments.** We acknowledge the use of data from ACE and GOES plasma and magnetic field experiments teams. This work was supported by grants NNSFC 40921063, 40831060, and 40911120062 and in part by the Specialized Research Fund for State Key Laboratories of China.

[27] Philippa Browning thanks the reviewers for their assistance in evaluating this paper.

References

Andréeová, K., and L. Přech (2007), Propagation of interplanetary shocks into the Earth's magnetosphere, *Adv. Space Res.*, *40*, 1871–1880, doi:10.1016/j.asr.2007.04.079.

Andréeová, K., T. I. Pulkkinen, T. V. Laitinen, and L. Přech (2008), Shock propagation in the magnetosphere: Observations and MHD simulations compared, *J. Geophys. Res.*, *113*, A09224, doi:10.1029/2008JA013350.

Collela, P., and P. R. Woodward (1984), The piecewise parabolic method (PPM) for gas-dynamical simulations, *J. Comput. Phys.*, *54*, 174–201.

Grib, S. A., B. E. Brunelli, M. Dryer, and W..-W. Shen (1979), Interaction of interplanetary shock waves with the bow shock-magnetopause system, *J. Geophys. Res.*, *84*(A10), 5907–5921, doi:10.1029/JA084iA10p05907.

Hu, Y. Q., X. C. Guo, and C. Wang (2007), On the ionospheric and reconnection potentials of the Earth: Results from global MHD simulations, *J. Geophys. Res.*, *112*, A07215, doi:10.1029/2006JA012145.

Li, X. L., D. N. Baker, S. Elkington, M. Temerin, G. D. Reeves, R. D. Belian, J. B. Blake, H. J. Singer, W. Peria, and G. Parks (2003), Energetic particle injections in the inner magnetosphere as a response to an interplanetary shock, *J. Atmos. Sol. Terr. Phys.*, *65*, 233–244.

Ridley, A. J., D. L. De Zeeuw, W. B. Manchester, and K. C. Hansen (2006), The magnetospheric and ionospheric response to a very strong interplanetary shock and coronal mass ejection, *Adv. Space Res.*, *38*, 263–272.

Samsonov, A. A., D. G. Sibeck, and J. Imber (2007), MHD simulation for the interaction of an interplanetary shock with the Earth's magnetosphere, *J. Geophys. Res.*, *112*, A12220, doi:10.1029/2007JA012627.

Shen, W. W. (1973), Interaction of interplanetary MHD shock waves with the magnetopause, *Astrophys. Space Sci.*, *24*, 51–64.

Shue, J.-H., J. K. Chao, H. C. Fu, C. T. Russell, P. Song, K. K. Khurana, and H. J. Singer (1997), A new functional form to study the solar wind control of the magnetopause size and shape, *J. Geophys. Res.*, *102*(A5), 9497–9511, doi:10.1029/97JA00196.

Tamao, T. (1964), The structure of three-dimensional hydromagnetic waves in a uniform cold plasma, *J. Geomagn. Geoelectr.*, *18*, 89–114.

Wang, C., J. B. Liu, H. Li, Z. H. Huang, J. D. Richardson, and J. R. Kan (2009), Geospace magnetic field responses to interplanetary shocks, *J. Geophys. Res.*, *114*, A05211, doi:10.1029/2008JA013794.

Wang, C., T. R. Sun, X. C. Guo, and J. D. Richardson (2010), Case study of nightside magnetospheric magnetic field response to interplanetary shocks, *J. Geophys. Res.*, *115*, A10247, doi:10.1029/2010JA015451.

Zhuang, H. C., C. T. Russell, E. J. Smith, and J. T. Gosling (1981), Three-dimensional interaction of interplanetary shock waves with the bow shock and magnetopause: A comparison of theory with ISEE observations, *J. Geophys. Res.*, *86*, 5590–5600.

X. C. Guo, H. Li, T. R. Sun, and C. Wang, State Key Laboratory of Space Weather, Center for Space Science and Applied Research, Chinese Academy of Sciences, Beijing 100080, China. (trsun@spaceweather.ac.cn; cw@spaceweather.ac.cn)